Welding Research

Sponsored by the Welding Research Council of the Engineering Foundation

WRC

SUPPLEMENT TO THE WELDING JOURNAL, DECEMBER 1971

# Cracking in Welded Steam Pipe

## Cracking tends to occur in a new grade of austenitic stainless (Fe-Ni-Cr-Mn-No-V-N-B) when the carbon content exceeds 0.030% and when noncircular inclusions are present

BY J. A. ISASI, R. C. BATES, AND J. HEUSCHKEL

### Introduction

The electrical industry continually faces demands for increased power generation. This demand is accompanied by a need for increased reliability of operations. During the past several decades, these conditions have led to progressive increases in steam temperatures and pressures. As a result, welded material characteristics have become one limiting factor in the industrial growth pattern. Early experiences with graphitization in Fe-Mo-C steels focused attention upon the needs for improvements in the ferritic steels. This led to the adoption of Cr-Mo steels for steam piping. Austenitic steels were next used to provide higher strength piping installations. Some unfavorable experiences were encountered with the AISI 347 Columbium-bearing grade. AISI 316 (Fe-Cr-Ni-Mo) has proven satisfactory in service but its strength at steam temperatures is low.

To provide a high strength, ductile, stable, fully austenitic, welded steam piping system, a new Fe-Ni-Cr-Mn-Mo-V-N-B alloy was developed.[1, 2] However, in power plant use, some cracking was experienced in high carbon content welded components which were fabricated by welding formed plates together.[3] The cracking which occurred was located primarily in the heat-affected zone immediately adjacent to the weld metal, but it sometimes occurred in the weld metal.

Recognizing the importance of the problem, a power plant surveillance program was initiated in 1969. In that program, field inspection teams developed and applied techniques for on-site radiography of welds, using iridium 192. This procedure revealed the presence of three of the internal, partial-depth cracks described in this paper. The surveillance system also included determining the circularity of components, a factor which strongly influenced stress levels based on pressure.[4]

The study being reported herein reveals that cracking occurrence was limited to those lots of plates containing more than 0.030% carbon; that cracking was influenced by the presence of noncircular components, which resulted in local stress risers;[4] and also by the presence of in-fabrication weld repairs, wherein the heat-affected zones were exposed to one or more additional high-temperature thermal cycles. Under service elevated temperature (1050F) tensile stress conditions, this combination of circumstances resulted in localized grain boundary stress-rupture cracks. In a few instances, these local cracks eventually extended through elbow or pipe walls, permitting steam leakage.

### Manufacturing History

#### Plates

The first production plate was fabricated from heats melted in 5000-lb capacity air induction furnaces. The ingots were forged into billets and the billets were hot-rolled into plates by subcontracting steel plants. Some larger heats were made in electric arc furnaces. After rolling the plates were annealed between 1550

MR. ISASI is Senior Engineer, Materials Engineering Laboratory, Large Turbine Div., Westinghouse Electric Corp., Philadelphia; Mr. Bates is Manager, Metals Application Research, Research & Development Center, Westinghouse, Pittsburgh; and Mr. Heuschkel is with the Metals Joining Research, Research & Development Center, Westinghouse Electric Corp., Pittsburgh.

This paper was presented at the AWS annual meeting in San Francisco, April 1971.

and 1700F. Current heats are being vacuum melted to meet a 0.020% maximum carbon content and improved cleanliness limits.

The two half-plates from which each elbow was made were cold formed in a closed die. The matching edges, taken from the same parent plate, were prepared by plasma-arc torch cutting, grinding, machining, or a combination thereof, to produce the joint geometry shown in Fig. 1. Any torch cutting was followed by grinding or machining to remove scale and oxides, and to provide a good fit.

The procedure described was used because no vendor was found who could produce large (10.75 to 16 in.) diameter thin-walled seamless elbows.

During the program described, the original permitted maximum plate carbon content of 0.04% was progressively reduced to a 0.020% maximum limit.

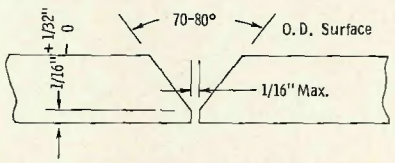


a. Prewelding Joint Geometry

b. Typical Weld Cross-Section (X 5) (Ground Flush Both Sides)

Fig. 1—Welded joint details

### Filler Wires

Bare wires for gas tungsten-arc (GTA) welding were produced from vacuum-melted heats. Over the life of the described program the maximum permitted filler wire carbon content was 0.020%. In the early part of the program, up to 0.20% Si was permitted in the filler wire but later that amount was reduced to 0.10%. In other respects the composition of the filler wire closely matched that of the base metal.

### Welding Procedures

Welding of the production elbows was performed over a period of about eight years but the same basic procedures were followed.

All welded edges were free of oil, grease, cutting fluids and other impurities. Surface areas adjacent to the weld edges were ground or polished back about 1 in. from the bevel, both O.D. and I.D. The part edges were then cleaned with acetone and/or alcohol.

The assembled, formed and annealed halves were tack welded together on the inside surfaces (root of the partial-depth V-groove) with about 1.5 in. long tacks spaced at about 6 in. centers; i.e., about 25% of the inner portions of both final welds were originally tack weld metal which was at least partially remelted. The helium-shielded tungsten-arc process was used for tacking, which was generally done without the use of filler metal; i.e., the tack welds had essentially the same composition as the base metal. The open-V side of the groove was backed up with helium gas during the tacking operations.

Starting and stopping run-out tabs were provided at both ends of every weld so that, except for the tack welds and any subsequent repairs, there were no arc starts or craters in the final welded components.

Before proceeding with welding, the elbow ends were sealed off with Plexiglass covers, attached with masking tape. Masking tape was also applied to the O.D. surfaces of the tacked longitudinal grooves. Each assembly was then purged for from 25 to 60 min with 15 cfh welding grade helium prior to the start of the final O.D. welding operation. Gas flow was continued throughout the first two root passes. This provided an inert gas back-up sufficiently pure that the weld root, including the original tack welds, were bright metal.

Elbows were welded while attached to a vertical face rotating positioner so that the weld was made in the flat position with the arc stationary and the piece moving. The longitudinal strips of masking tape were progressively pulled off just ahead of the moving arc.

The direct current, straight polarity welding was done with $^1/_8$ in. diam 1% thoriated electrodes machined to a sharp tip. Welding currents ranged from 150 to 200 amp, arc voltages from 12 to 15, and travel speeds from 4 to 7 ipm, depending upon the pass number.

With the described procedure, all the tack welds and the first full-length root pass consisted of remelted base metal, and essentially had the composition of the particular piece of base metal being welded. This meant that the carbon content, and other alloying elements, of the root pass varied as widely as the provided plate stock.

Following completion of the root fusion pass, the remainder of the groove was filled with the low carbon content filler metal already described. This resulted in a condition where the body of the weld usually had a lower carbon content than the I.D. weld root, depending upon the plate composition.

### Weld Repairs

Completed welds were subjected to a 100% low voltage X-ray examination. Observed defects including spherical porosity as small as 0.03 in. diam were removed by grinding and those regions were manually rewelded. Since the flaws were sometimes found in the root pass, this often resulted in making relatively deep grooves from 2 to 4 in. long for rewelding. Sometimes upon re-X-ray examination new flaws were observed. This necessitated additional regrinding and rewelding. Thus some regions in some components were subject to several high temperature thermal-stress cycles.

In some instances the final surface grinding of the O.D. and I.D. resulted in thinning of the wall below allowable limits. This resulted in some weld overlays being applied to rebuild the wall thicknesses up to acceptable limits. This, too, resulted in the local metal being subject to additional temperature-stress cycles.

These points are emphasized because the investigation showed that most field cracks detected occurred in components that had been rewelded during initial fabrication. One largely unanswered question is whether or not the in-service detected cracks were present from the beginning.

Some of the observed variations in final weld cross-sections are shown in Fig. 2

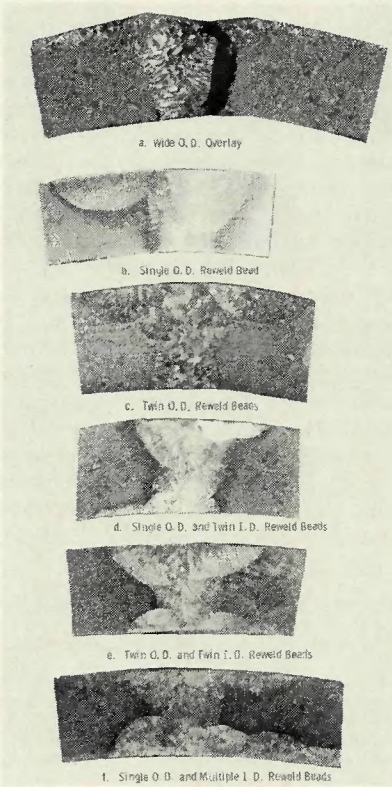


Fig. 2—Range of elbow weld anomalies. Mag: 5X

## Investigative Procedures

In parallel with the efforts of the plant surveillance teams, a study was made to isolate and identify the causes of the field cracking experienced. This involved the accumulation of cracked and uncracked service exposed components for nondestructive examinations, identification of sources of materials, obtaining welding histories, and making fractographic examinations; and making destructive chemical, macrographic, micrographic, sensitization and physical property evaluations.

### Specimen Selection

Twelve cracked and uncracked elbows and one piece of straight pipe taken from five installations were examined. Typical examples are discussed. For purposes of identification, the installation samples are indicated in chart A.

Production records included the heat number and the melting source of every incident elbow component. Also it was possible in most cases to obtain the original welding history on each part. It was not possible, however, to identify the heat from which the section of straight pipe was manufactured.

### Nondestructive Tests

Cut-out segments and complete elbows, removed from cracked and uncracked service installations, were nondestructively X-ray examined in the laboratory to determine the locations of internal and external cracks, if any. The X-ray films also showed the presence of weld repair regions. These appear on the film as wide volumes of weld metal. X-ray conditions were: 60 in. source to film distance and 14 min exposure at 10MA and 140KV on Eastman "M" film.

Fractographic examinations were made on fracture surfaces in several instances.

### Destructive Tests

Test samples were taken so that both plate components of each elbow were examined for critical element chemical composition, macrographic and micrographic examinations, Strauss tests, and tensile and stress rupture tests. Millings for carbon analyses were taken from the I.D. and O.D. surfaces at 5-mil depth increments to establish the presence or absence of carbon gradients. Other through-depth millings were taken so that those samples represented the average through-thickness of the plate material.

From 3 to 30 macrographic samples were taken from each intrados or extrados weld from each elbow examined. This provided a reasonably accurate revelation of the quality of the welds. Most specimens were taken from those joints showing maximum likelihood of deviations from standard weld geometries.

Selected macrographic specimens were polished and examined to reveal details of the microstructure of the weld metal, weld heat-affected zones, and unaffected plate materials.

Strauss test specimens of essentially the same size and arrangement as the transweld macrographic specimens were made. One such specimen was taken for each weld investigated.

One-inch wide transverse joint stress-rupture and tensile specimens were made across representative low and high carbon content plate joints.

**Chart A—Installation Samples**

| Installation No. | Component | Cracking | Plate Heat No. | Location of Crack |
|---|---|---|---|---|
| 1 | El. 1 | Yes | 806286 | intrados |
| 1 | El. 12 | Yes | 806286 | intrados |
| 2 | El. 12 | Yes | 806286 | intrados |
| 4 | El. 7 | Yes | 806286 | [a] |
| 4 | El. 8 | Yes | 806286 | [a] |
| 3 | El. 1 | Yes | 2813 | intrados |
| 3 | El. 12 | No | 2813 | — |
| 3 | El. 2 | [b] | 2569 | intrados[b] |
| 3 | El. 7 | No | 2819 | — |
| 3 | El. 8 | No | 2809 | — |
| 3 | El. 11 | No | 2837 | — |
| 3 | st. pipe reheat no. 2 | Yes | unknown | weld edge |
| 5 | El. 10 | [c] | 2696 | extrados |

[a] At junction of intrados welds and circumferential weld
[b] Running crack originating in elbow No. 1
[c] Manufacturing defect; did not propogate in service.

## Results of Tests

### Chemical Analyses

The first step in establishing cause and effect relationships was to verify the actual compositions of the incident components. This was followed by the same type determinations for a series of other heats, and to a lesser extent for nonincident components. The analyses determined are shown in Table 1 and 2.

The most significant deviation between originally reported ladle analysis and the newly determined check analysis was found in carbon contents, Fig. 3. The heats which resulted in field cracking were highest in carbon content and the check analyses were higher than the previously reported ladle analyses.

In almost every case the surface 5-mil layer contained slightly more carbon than each of the underlying layers. The highest individual uncracked elbow surface 5-mil layer carbon content observed was 0.078%. The average carbon content obtained from these four uncracked elbow surface samples was 0.058%, while the average of the four subsurface layers in those units was 0.050%. Carbon analyses from samples which average the full depth of the pipe wall were similar to those obtained from the four 5-mil subsurface layers, that is, the center of the plate had about the same composition (av. = 0.055%) as the outer subsurface portions (av. = 0.050%).

These observations lead to the circumstantial conclusion that surface carburization was not a significant contributing factor in the observed cracking.

To obtain accurate nitrogen analyses, it was found that the field exposed materials must first be solution heat treated to about 2100F. This is an indication that some of the nitrogen was converted into a nonsoluble form during service. The nitrogen contents then ranged up to 0.196% by weight.

For V, N, and B, good agreement was found between check and ladle analyses. The Zr content was somewhat lower and the Si content was significantly lower on check analysis, compared with the reported ladle analyses.

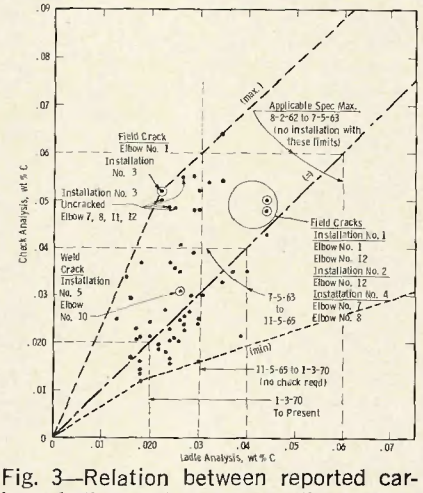


Fig. 3—Relation between reported carbon ladle analyses and elbow plate stock check analyses

**Table 1—Chemical Analyses (wt %) of Ladle Button, Plates, and Weld Metals From Installations No. 1, 2 and 4. (Heat 806286)**

| Material | Ladle analysis button | | Plates | | | Weld metals | | | | | |
|---|---|---|---|---|---|---|---|---|---|---|---|
| Determination | Original | Recheck | Check | | | Check | | | | | |
| Installation no. | 1, 2 & 4 | 1, 2 & 4 | 1, 2 & 4 | | | 1 | | | | 2 | |
| Elbow no. | — | — | 1, 2 & 12 | | | 1 | 2 | | | 12 | |
| Location | — | — | Min | Max | Avg | Extrados OD | Extrados OD | Intrados ID | Intrados OD | Extrados ID | Extrados OD |
| carbon | 0.044 | 0.048 | 0.048 | 0.057 | 0.053 | 0.017 | 0.021 | — | — | 0.032 | 0.032 |
| manganese | 9.30 | 9.85 | 7.50 | 9.70 | 8.62 | 10.3 | 10.1 | — | — | 9.63 | 9.57 |
| phosphorus | 0.018 | 0.012 | 0.006 | 0.012 | 0.009 | 0.009 | 0.010 | — | — | 0.005 | 0.005 |
| sulphur | 0.012 | — | 0.0083 | 0.016 | 0.0134 | 0.009 | 0.0098 | — | — | 0.009 | 0.011 |
| silicon | 0.24 | 0.22 | 0.09 | 0.23 | 0.19 | — | — | — | — | 0.20 | 0.15 |
| copper | — | 0.11 | 0.10 | 0.11 | 0.11 | — | — | — | — | — | — |
| nickel | 20.82 | 20.7 | 20.1 | 20.78 | 20.40 | 21.6 | 21.3 | — | — | 20.75 | 21.00 |
| chromium | 15.16 | 15.4 | 14.12 | 15.4 | 14.75 | 15.5 | 15.3 | — | — | 15.20 | 15.40 |
| molybdenum | 1.96 | 2.03 | 1.75 | 2.04 | 1.86 | 2.14 | 2.17 | — | — | 2.06 | 2.02 |
| vanadium | 0.24 | 0.20 | 0.18 | 0.24 | 0.20 | 0.26 | 0.27 | — | — | 0.20 | 0.20 |
| zirconium | 0.006 | 0.0052 | 0.003 | 0.013 | 0.0055 | 0.004 | 0.009 | 0.001 | <0.001 | <0.001 | 0.003 |
| boron | 0.015 | — | <0.002 | 0.0176 | 0.012 | 0.0098 | 0.0098 | 0.015 | 0.016 | 0.013 | 0.014 |
| nitrogen | 0.16 | 0.158 | 0.072 | 0.129 | 0.100 | 0.18 | 0.21 | — | — | — | — |
| oxygen | — | 0.0090 | 0.0052 | 0.0092 | 0.0071 | — | — | — | — | — | — |
| hydrogen | — | — | 0.00002 | 0.00006 | 0.00003 | — | — | — | — | — | — |
| aluminum | — | — | — | — | — | — | — | 0.014 | 0.012 | 0.013 | 0.015 |

**Table 2—Chemical Analyses (wt %) of Ladle Button, Plates, and Weld Metals From Installations No. 3 and 5. (Heat Nos. 2813, 2569, and 2696)**

| Material | Ladle analysis button | | Plates | | | | | | | Weld metals | | | | |
|---|---|---|---|---|---|---|---|---|---|---|---|---|---|---|
| Determination | Original | Recheck | Check | | | Ladle | Check | Ladle | Check | Check | Check | | | |
| Installation no. | 3 | 3 | 3 | | | 3 | 3 | 5 | 5 | 3 | 3 | | | |
| Heat no. | 2813 | 2813 | 2813 | 2813 | 2813 | 2569 | 2569 | 2696 | 2696 | unknown | 2813 | | | |
| Elbow no. | 1 | 1 | 1 | 1 | 1 | 2 | 2 | 10 | 10 | st. pipe | 1 | 1 | 1 | 1 |
| Location | — | — | Min | Max | Avg | — | Avg | — | Avg | — | ID Intrados | ID Extrados | OD Intrados | OD Extrados |
| carbon | 0.022 | 0.025 | 0.050 | 0.063 | 0.056 | 0.013 | 0.012 | 0.025 | 0.031 | | 0.045 | 0.050 | 0.028 | 0.026 |
| manganese | 10.8 | 11.36 | 11.0 | 10.06 | 10.38 | 10.8 | 11.1 | 10.4 | 9.8 | | | | | |
| phosphorus | 0.005 | 0.009 | 0.006 | 0.011 | 0.008 | 0.006 | 0.005 | 0.004 | 0.008 | | | | | |
| sulphur | 0.005 | 0.0085 | 0.007 | 0.010 | 0.009 | 0.009 | 0.0087 | 0.005 | 0.013 | | | | | |
| silicon | <0.05 | .0.031 | <0.01 | 0.08 | 0.036 | 0.03 | 0.020 | 0.09 | 0.04 | | | | | |
| copper | — | 0.018 | 0.018 | 0.020 | 0.019 | — | 0.017 | — | — | | | | | |
| nickel | 21.1 | 20.7 | 20.3 | 21.25 | 20.77 | 20.9 | 21.1 | 21.2 | 20.7 | | | | | |
| chromium | 15.6 | 15.4 | 14.60 | 15.4 | 15.05 | 15.9 | 15.6 | 15.2 | 15.4 | | | | | |
| molybdenum | 2.20 | 2.03 | 1.96 | 2.49 | 2.11 | 2.30 | 2.35 | 2.19 | 2.15 | | | | | |
| vanadium | 0.16 | 0.15 | 0.07 | 0.18 | 0.147 | 0.21 | 0.21 | 0.18 | 0.20 | | | | | |
| zirconium | 0.010 | 0.014 | 0.01 | 0.016 | 0.012 | 0.004 | 0.0041 | 0.006 | 0.001 | | 0.010 | | 0.018 | |
| boron | 0.011 | 0.0068 | 0.007 | 0.013 | 0.010 | 0.004 | 0.0040 | 0.004 | 0.01 | | 0.013 | | 0.011 | |
| nitrogen | 0.16 | 0.189 | 0.117 | 0.219 | 0.152 | 0.15 | 0.143 | 0.15 | 0.13 | | | | | |
| oxygen | — | — | 0.0071 | 0.0190 | 0.0100 | — | 0.0102 | — | — | | | | | |
| hydrogen | — | — | 0.00010 | 0.00014 | 0.00012 | — | 0.00007 | — | — | | | | | |
| aluminum | — | — | <0.005 | 0.01 | <0.005 | — | — | — | — | | | | | |

### Visual and Macroscopic Examinations

Several of the cracks in cracked elbows were opened, and the fracture surfaces were examined visually and with a low power binocular microscope. Many features of most of the cracks in those elbows manufactured from high (>0.048%C) carbon material were similar. With the exception of the crack in the elbow made from Heat No. 2696 (containing 0.031%C), the initial portions of the cracks were intergranular and heavily oxidized. Generally the degree of oxidation appeared to decrease as the distance from the origins increased, indicating that the cracks were propagating in service, however slowly. Multiple cracking was typical, although in many instances two or more cracks had joined to form, in effect, a single crack. Crack initiation appeared to be subsurface, but near the I.D., judging from a prevalence of tiny shear lips along the I.D. surfaces and large shear lips at the O.D. surface (in those cases where the cracks penetrated to the O.D. surface). The ratio of crack depth to crack length for each individual crack was determined, where possible. Generally this ratio was greatest for the smallest cracks, indicating that the lateral crack growth rate (along the I.D. surface) was generally higher than the rate of crack growth through the walls.

An extrados crack in the elbow made from Heat 2696 was significantly different from those examined in other elbows. This crack appeared to be completely internal and did not penetrate to either surface, although a dimple was formed on the I.D. surface from necking of the material between the internal crack and the surface, see Fig. 4a. Verification that the crack did not penetrate to the surface was obtained from fluorescent penetrant testing.

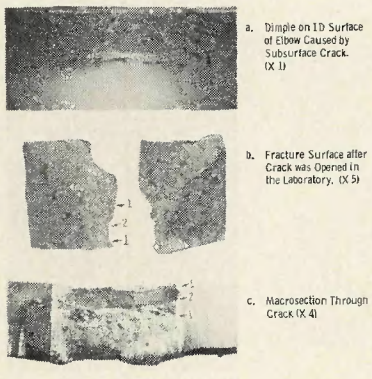


Fig. 4—Crack and associated surface dimple in Elbow No. 10, Installation No. 5 (heat 2696) (Portions marked 1 broken in lab and that marked 2 is original crack)

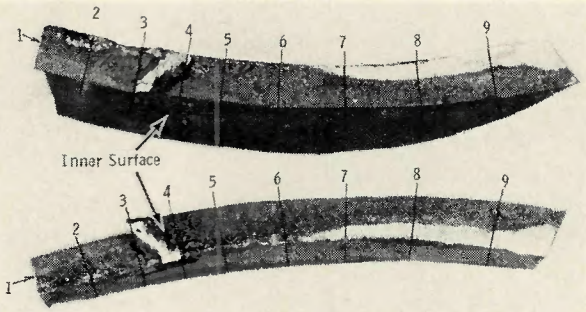


Fig. 5—Photographs of fracture surfaces in elbow no. 12, installation no. 1, showing locations of metallographic sections and fracture replicas. Mag: 2X

The crack was opened and examined visually (see Fig. 4b) and found to be approximately 3/4-in. long and 0.080-in. deep. Its nearest approach to the I.D. surface was about 0.050 in. Even though this crack was completely subsurface, it appeared heavily oxidized. The oxide was uniform in appearance, even near the boundaries, indicating that crack propagation had not occurred in service and that it had formed during welding.

The full-depth cracks in several of the elbows and in the one straight pipe section were not opened. This permitted making complete sections through the cracked welds for macroscopic and metallographic examinations. In those cases in which the cracks were opened, sections were also made through the adjacent weld and base metal. In these instances, mating sections from opposite sides of the cracks were matched to the extent possible. The locations of sections through one of the cracks and several low magnification photographs of the macroetch specimens are shown in Figs. 5, 6, 7, and 8. In general, sections were cut at about 1/2-in. intervals through all cracked portions of the elbows.

The cracks in the straight pipe sections and those in most of the elbows initiated adjacent to the welds in the heat-affected zones of the base metal, although some weld metal cracks were also found, especially in the straight pipe section at sharp notches on the I.D. surface. In one instance, Elbow No. 12, Installation No. 2, the cracking was contained principally in the weld metal. Evidently, part of the difference in this case was the presence of extensive I.D. weld repairs, which were made during initial fabrication of the elbows.

Inside diameter rewelding and heavy outside diameter weld overlays were present in all cracked elbows. Almost all cracks could be associated with these regions. An exception was an intrados crack in the vicinity of the intersection of a circumferential weld joining elbows 7 and 8 in Installation No. 4. In this case, cracking was confined to the area immediately adjacent to the intersection.

Two sections were taken through the crack in Elbow No. 10, Installation No. 5, and prepared for macrographic and metallographic examinations. The macroscopic examination of these two sections revealed that no weld repair had been made in the vicinity of the crack. The crack was confined to the root portion of the weld metal, Fig. 4c. This crack appears not to be connected to the I.D. surface, but it does appear to have intersected the top of the root pass so that it could have been exposed to the external environment until weld filler metal was deposited over it.

Macrographs were taken from each uncracked elbow and uncracked portions of cracked elbows. These sections were examined so that a record of the weld configurations would be available. Several of the uncracked macrosections are shown in Fig. 9.

In contrast to the cracked welds, the uncracked welds contained no O.D. weld repairs in the areas examined. A few areas were observed in which deposits of weld metal were present at the I.D., indicating that some I. D. weld repairs had been made.

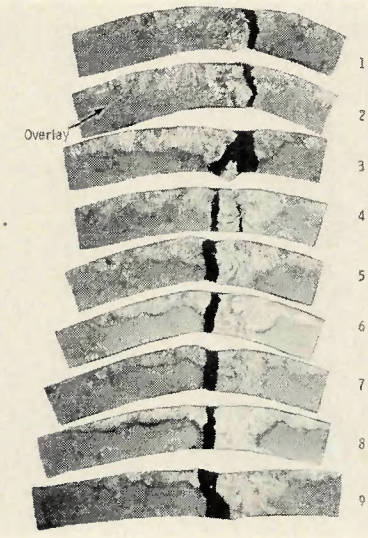


Fig. 6—Macrographic sections through fractures in elbow no. 12, installation no. 1. Numbers indicate location as shown in Fig. 5. Mag: 2X

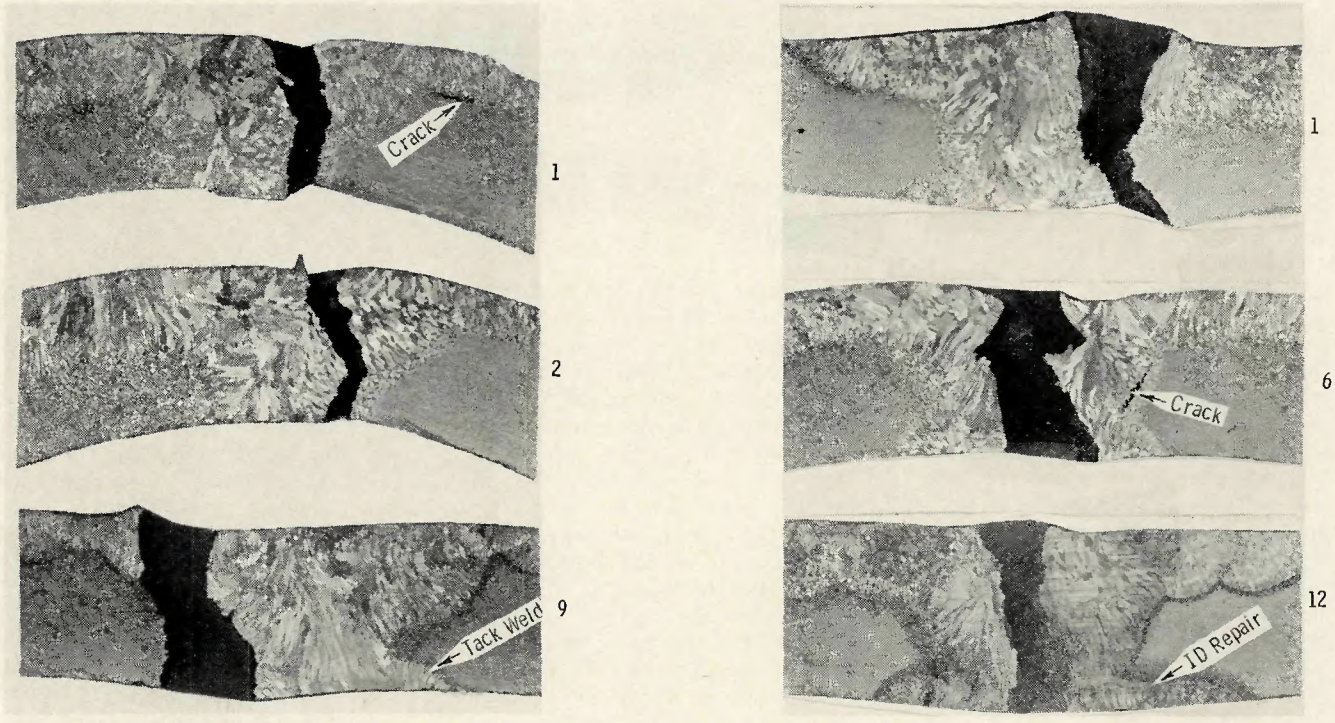


Elbow No. 12, Installation No. 1

Elbow No. 12, Installation No. 2

Fig. 7—Selected macrographs of cracked welds. Mag: 3.25

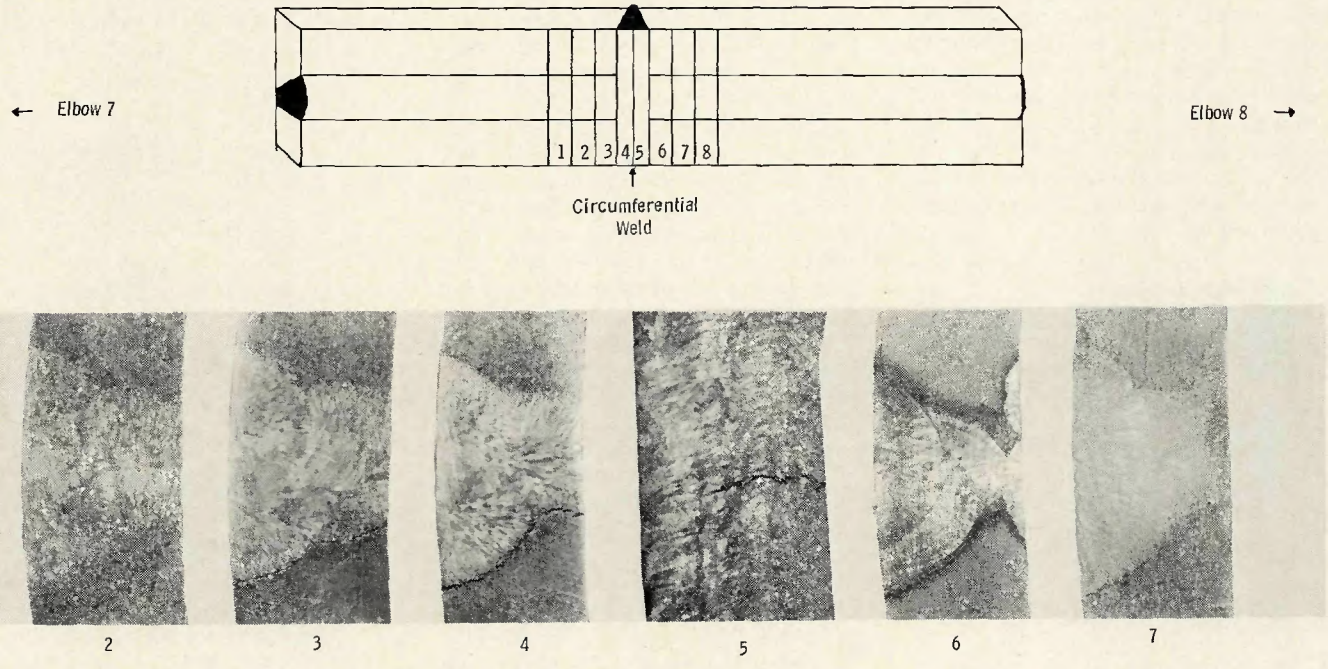


Fig. 8—Macrosections through cracked intrados welds in installation no. 4. Mag: 5X

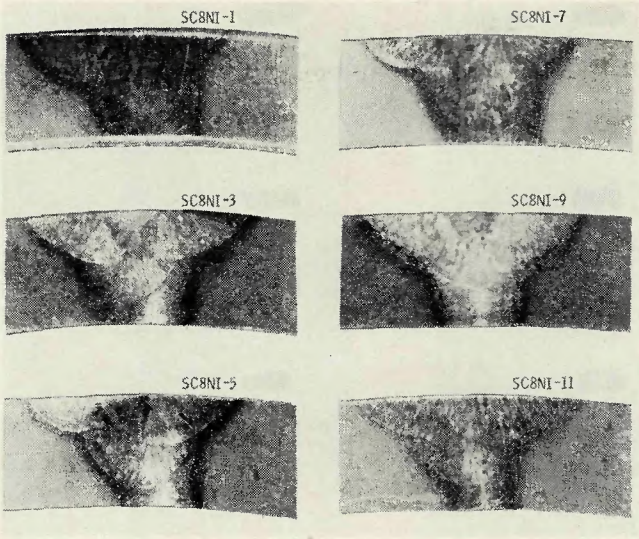


Fig. 9—Macrosections of intrados welds in elbow no. 8, installation no. 4. Mag: 5X

## Metallographic Examinations

The microstructure of the plate material after heat treatment for one hour at 1700F following hot rolling has been described previously as consisting of a recrystallized medium-fine grain size with a dispersion of fine precipitates present in the prior grain boundaries and within the grains.[2] Large spheroidal and relatively fine particles are present at the grain boundaries. The large spheroidal particles at the boundaries were identified as $Cr_2N$ and the fine intergranular particles as $Mn_4N$ and $M_6C$. In addition, a very fine intragranular precipitate, tentatively identified as $VN_x$, forms during creep testing and is partially responsible for the good properties of the material which make this alloy both a solution hardening and a precipitation hardening austenitic steel. The microstructure (grain size and type, size, distribution, and relative amount of precipitates) will strongly depend on composition, grain size prior to final working, final working temperature, amount of deformation during final working, and heat treatment following final working.

To provide some background information concerning the original microstructure of the elbows of concern in this investigation, unused plate samples from Heat No. 806286 were examined, Fig. 10a. Also, samples taken from a creep specimen made from either plate material or from a trimmed end of elbows (transweld creep specimens) were examined. Figures 10b and 11 give the typical microstructure for these two types of specimens.

### Service Exposed Material

The microstructure of all cracked material (elbows and straight pipe) and of uncracked material (elbows) were examined by optical and electron metallographic techniques.

*(a) Material from Installations Nos. 1, 2, 3, and 4.* In all cracked components examined the heavily oxidized portions of the cracks were intergranular. Intergranular secondary cracking (near but isolated from the main crack) and branch cracking were common. About half of the components (elbows and straight pipe) examined contained cracks which had completely penetrated the wall. The final portions of the material to separate (near the O.D. surface) exhibited appreciable ductility and the cracks in these areas consisted of a mixture of intergranular and transgranular features, Fig. 12. For the components in which the crack was opened in the laboratory, the portion broken in the laboratory (near O.D.) was principally transgranular. Typical microstructures at different positions along the wall thickness are shown in Figs. 12, 13, and 14.

For all cracked components except Elbow No. 12, Installation No. 2, the crack was restricted to the heat-affected zone either at the interface between the HAZ and the weld or one or two grains away from it. For Elbow No. 12, Installation No. 2, most of the crack path was confined to the weld region with the exception of small portions of the crack. In those small portions, the cracking was in the HAZ and it resembled the HAZ cracks in the other components.

The microstructures of the base metal in all cracked components investigated were found to be approximately the same, showing a recrystallized medium size grain structure, with a few large intermixed grains. The width of the HAZ was determined to be up to 0.03 in. wide and to contain large sized grains (up to 0.005 in.) in all four of the cracked elbows investigated.

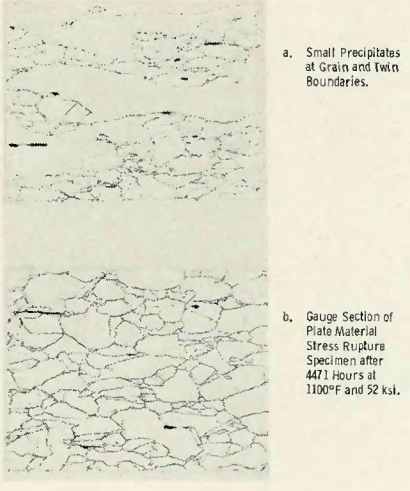


Fig. 10—Microstructure of original plate in as-heat-treated condition and after stress-rupture tests made from heat no. 806286. Mag: 1000X

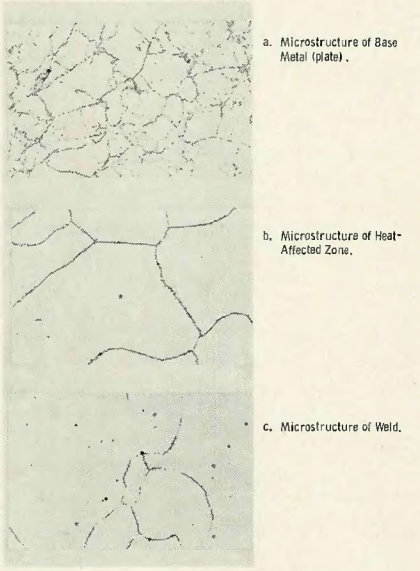


Fig. 11—Typical microstructure of three areas in transweld creep-rupture specimen (weld at center of gauge length) after 7843 hr at 1025F and 50 ksi. Specimen machined from trim end of 14-in. elbow made from heat no. 806286. Mag: 1000X

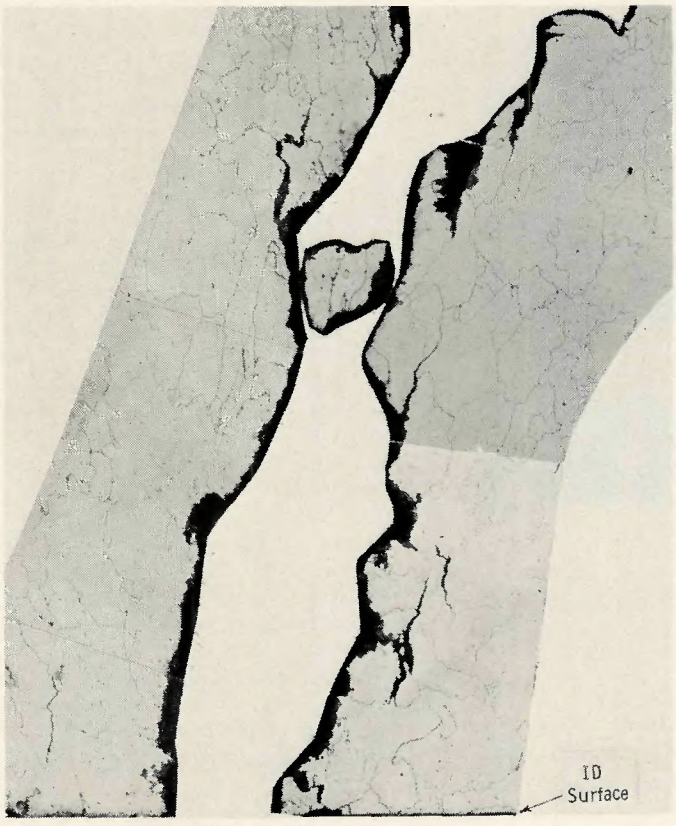


a. Section Near ID Surface of Pipe

b. Section Showing Part of OD Weld Bead.

Fig. 12—Microstructure of area containing crack in elbow no. 12, installation no. 2. Mag: 100X

Fig. 13—Microstructure of area containing crack in elbow no. 1, installation no. 3. Mag: 100X

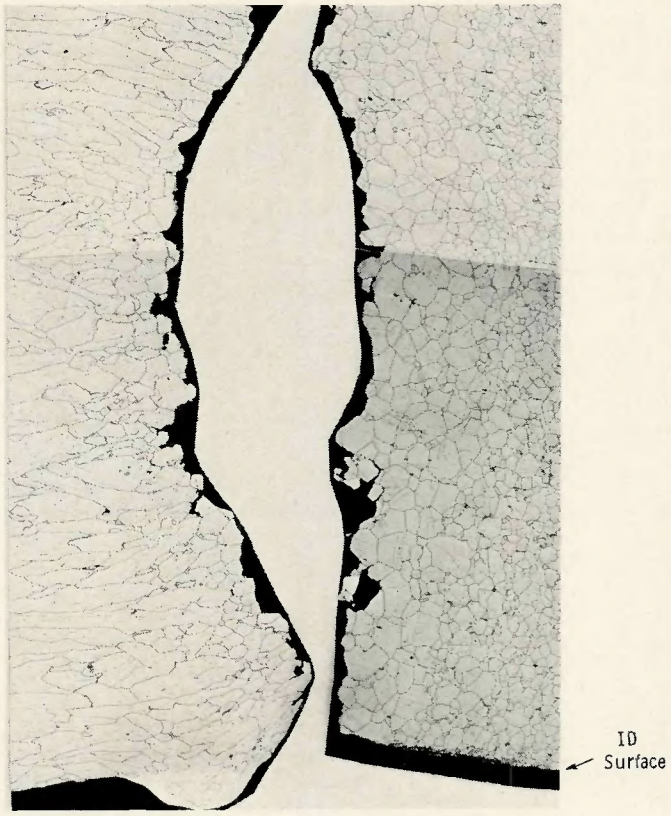


a. Section Near ID Surface of Pipe.

b. Section Showing Part of OD Weld Bead.

Fig. 14—Typical microstructure at mid-depth of straight pipe, installation no. 3, showing crack. Mag: 100X

The microstructures of all investigated components except Elbow No. 2, Installation No. 3, were found to contain large amounts of precipitates as illustrated in Figs. 15 and 16. The relative distribution of particles in these components was determined to be about the same. In the base metal, the particles were located primarily at the grain boundaries, twin boundaries, and prior boundaries, with small amounts situated randomly within the grains. In the HAZ and weld regions, the particles were found mainly at the grain boundaries; although small amounts of fine intragranular precipitates were present in the weld which appear to be associated with the dendritic structure. In general, the size of the particles in the HAZ and weld areas were much larger than in the base metal and form essentially a continuous network at the boundaries.

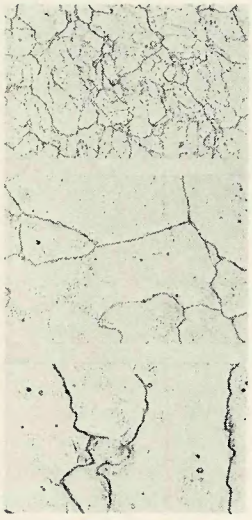


Fig. 15—Typical microstructure of three areas in elbow no. 12, installation no. 2. Elbow made from heat no. 806286. Mag: 1000X

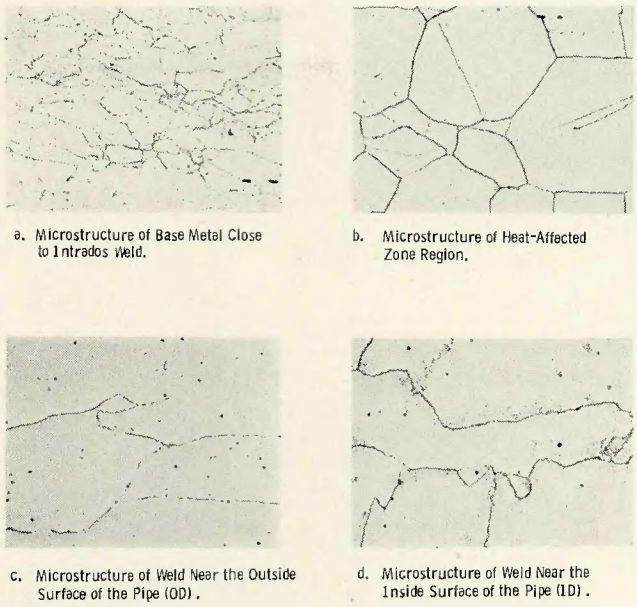


Fig. 16—Typical microstructures of three areas in elbow no. 1, installation no. 3 Elbow made from heat 2813. Mag: 1000X

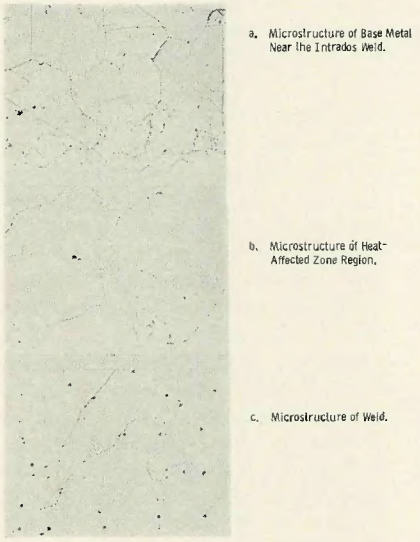


Fig. 17—Typical microstructure of three areas in elbow no. 2, installation no. 3. Elbow made from heat 2569. Mag: 1000X

For most of the components under investigation, two different regions could be clearly observed in some of the metallographic sections of the weld areas. This is illustrated for Elbow No. 1, Installation No. 3, in Fig. 16c and d. The microstructure of the weld region (0.028%C) close to the O.D. surface of the pipe was found to be almost free of particles, as shown in Fig. 15c. The second region corresponding to the area of the root pass of the weld (i.e., close to the I. D. surface of the pipe) was found to contain large particles at the grain boundaries and fine particles in the grains close to the boundaries, as shown in Fig. 16d. The reason for the differences in the two regions is that close to the I.D. surface of the pipe the carbon content was approximately the same as that of the plate (high carbon), and the region close to the O.D. contained approximately the same amount of carbon as the low (0.02%) carbon welding wire which was used.

Elbow No. 2 of Installation No. 3 was the companion to Elbow No. 1; therefore, both elbows were exposed to the same service condition. Elbow No. 2 was made from Heat No. 2569 (0.012% carbon). A direct comparison of the microstructure of Elbow No. 2, Fig. 17, to that of Elbow No. 1 (0.053%C), Fig. 16, indicates the effect of service exposure on the microstructure of material having different carbon levels.

Figure 18 shows electron micrographs at 5000X from plastic replicas illustrating the amount and morphology of the grain boundary particles in the original plate material from Heat No. 806286 and in a typical elbow made from that heat after service. These electron micrographs clearly illustrate the effect of service conditions on the microstructure of the material, i.e., precipitation of particles during service. Carbon extraction replicas from the base material of all four elbows investigated were obtained and used to identify the grain boundary particles by electron diffraction and electron microprobe analyses of single large particles or groups of particles. The particles were identified to be mostly $M_{23}$ $C_6$ type carbide (where M is mainly Cr) plus possibly some Cr-Mo-N and Cr-N particles. Strong indication of nitrogen substitution for carbon in $M_{23}C_6$ type carbide was also detected. The presence of a large number of $M_{23}C_6$ type particles at

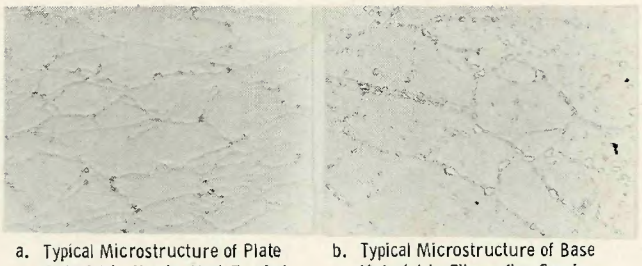

a. Typical Microstructure of Plate Material in the As-Heat-Treated Condition, Made from Heat 806286.

b. Typical Microstructure of Base Material in Elbow after Service. Note the Difference in Grain Structure and Amount and Distribution of Precipitates.

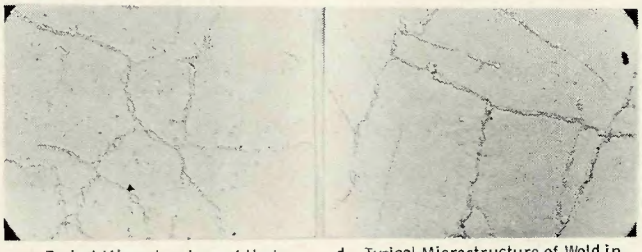

c. Typical Microstructure of Heat-Affected Zone in Elbow after Service. Note the Almost Continuous Grain Boundary Precipitate.

d. Typical Microstructure of Weld in Elbow, after Service. Note Almost Continuous Grain Boundry Precipitate.

Fig. 18—Electron micrograph from plastic replicas showing relative amounts, size, and distribution of precipitates in plate material before service and in plate material, HAZ, and weld after service (elbow no. 1, installation no. 1). Mag: 5000X

a. Micrograph Showing Transgranular Nature of the Crack

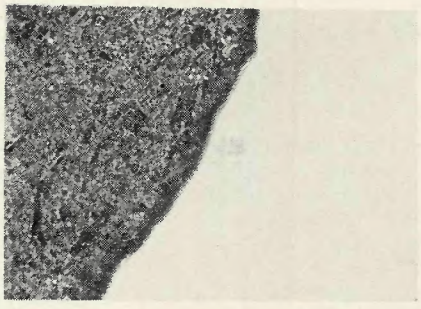

b. Micrograph Showing the Thin Oxide Layers on the Crack Surface. Unetched.

Fig. 20—Micrographs of a section containing crack from elbow 10, installation no. 5. Mag: 500X

the boundaries agrees well with previous observations in materials of similar composition.[1]

Because of the large amount of chromium carbide particles at the grain boundaries of service exposed elbows, transweld samples from each component examined were obtained and tested for susceptibility to intergranular attack. The test procedure chosen was the acidified copper sulfate (Strauss) test which will detect severe grain boundary precipitation of chromium carbides but in general will not detect sigma phase formation.

The results obtained from the Strauss test agree well with the microscopic observation showing that all areas with large amounts of precipitate (elbows from high carbon heats) were attacked. In all cases in which attack occurs, the maximum attack was at the HAZ. Figure 19 illustrates the appearance of two such specimens

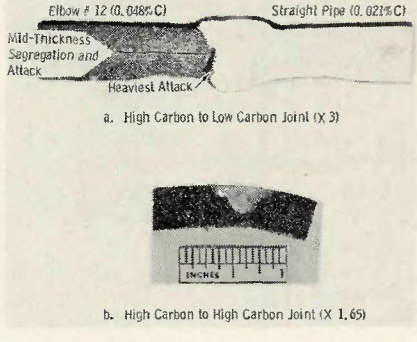


Fig. 19—Transweld specimens after 24 hr Strauss test (acidified copper sulphate solution)

*(b) Elbow No. 10, Installation No. 5.* For this component, the cracking was determined to be mostly transgranular and no evidence of secondary cracking nor branch cracks were found, Fig. 20a. In addition, a thin layer of oxides could be seen in the unetched condition, Fig. 20b. No evidence of cracking in the HAZ was observed. The portion of the crack formed in the laboratory while opening the defect for observation was principally transgranular.

The microstructure of this material was determined to be about the same as that of Elbow No. 2, Installation No. 3. The amount of grain boundary precipitate was slightly more than Elbow No. 2, Installation No. 3, but significantly less than that found in components manufactured from Heat Nos. 806286 or 2813.

## Mechanical Testing

The general mechanical properties of the plate material have been fully described previously.[2] In that publication, a study of the effects of several processing parameters on the mechanical properties of the alloy is presented.

### Tensile Data

Background information on the tensile properties of the material, and in particular of the heats used to manufacture the elbows under investigation, was compiled from records. Typical design values are presented in Table 3, togeher with the average results obtained from the service exposed elbows.

For all four heats studied, there appears to be no significant differences in room temperature yield strength and reduction-of-area for plate vs transweld specimens. The tensile strengths and elongations for the transweld specimens were found to be slightly lower and significantly lower, respectively, than for the base plate. A comparison of the typical room temperature tensile properties of as-fabricated elbows to the typical tensile properties of this material shows good agreement.

The average tensile data obtained on service exposed material are shown in Table 3, Section c. The base metal, and transweld tensile properties for Elbow Nos. 1 and 2, Installation No. 1, and Elbow No. 12, Installation No. 2, and Elbow Nos. 7 and 8, Installation No. 4 (Heat No. 806286) were found to be about the same; therefore, to simplify Table 4, they are grouped together. A comparison of the transweld tensile properties with those of the base metal for this heat shows that the tensile and fracture strength of base metal is higher than that of the weld metal. The yield strengths for both regions are about the same. The tensile data for Elbow Nos. 1 and 2 of Installation No. 3 (Heats 2813 and 2569) may be misleading due to the deformation introduced in the elbow following cracking. For most of the components investigated, the transweld ductility was lower than that of the plate specimen. In all cases, the ductility of

**Table 3—Standard Test Tensile Data**

| Material identification (heat no.) | Location of specimen | Test temp. °F | Average results* Y.S. (ksi) | T.S. (ksi) | F.S. (ksi) | Elong. % | R.A. % | Comments |
|---|---|---|---|---|---|---|---|---|
| *a) Typical values of the as-heat-treated conditions* | | | | | | | | |
| — | plate | RT | 55 | 110 | — | 45 | 68 | — |
| — | plate | 1050 | 38 | 78 | — | 40 | 53 | |
| *b) Specimen taken from as-fabricated elbows (before service)* | | | | | | | | |
| 806286 | plate | RT | 55 | 98 | — | 37 | 68 | |
| 2813 | plate | RT | 56 | 106 | — | 40 | 63 | — |
| 2569 | plate | RT | 56 | 102 | — | 41 | 67 | |
| 2696 | plate | RT | 54 | 100 | — | 40 | 60 | |
| 806286 | transweld | RT | 49 | 93 | — | 27 | 60 | |
| 2813 | transweld | RT | 60 | 95 | — | 26 | 66 | — |
| 2569 | transweld | RT | 58 | 93 | — | 26 | 55 | |
| 2696 | transweld | RT | 52 | 88 | — | 28 | 60 | |
| *c) Specimen taken from service-exposed elbows*** | | | | | | | | |
| 806286 | plate | RT | 54 | 103 | 182 | 35 | 50 | |
| 2813 | plate | RT | 53 | 106 | 205 | 33 | 55 | |
| 2813 | plate | RT | 51 | 103 | 182 | 30 | 51 | uncracked elbow |
| 2569 | plate | RT | 52 | 95 | 210 | 38 | 60 | |
| 2696 | plate | RT | 59 | 105 | 227 | 43 | 62 | |
| 806286 | transweld | RT | 50 | 90 | 105 | 14 | 40 | |
| 2813 | transweld | RT | 48 | 85 | 140 | 26 | 50 | |
| 2813 | transweld | RT | 54 | 92 | 151 | 14 | 38 | uncracked elbow |
| 2569 | transweld | RT | 50 | 91 | — | 28 | 58 | |
| — | transweld | RT | 62 | 105 | 139 | 19 | 28 | straight pipe |
| 806286 | plate | 1050 | 30 | 71 | 108 | 23 | 40 | |
| 2813 | plate | 1050 | 36 | 72 | 100 | 24 | 41 | |
| 2813 | plate | 1050 | 30 | 71 | 133 | 32 | 51 | uncracked elbow |
| 2569 | plate | 1050 | 41 | 73 | 130 | 29 | 49 | |
| 2696 | plate | 1050 | 45 | 73 | 134 | 35 | 55 | |
| 806286 | transweld | 1050 | 31 | 60 | 71 | 17 | 35 | |
| 2813 | transweld | 1050 | 28 | 58 | 90 | 18 | 40 | |
| 2813 | transweld | 1050 | 30 | 62 | 96 | 16 | 37 | uncracked elbow |
| 2569 | transweld | 1050 | 31 | 70 | — | 24 | 48 | |
| — | transweld | 1050 | 37 | 70 | 119 | 18 | 40 | straight pipe |

* Represents the average for 3 or more tests.
** All specimens from cracked components except as noted in right column.

**Table 4—Typical Stress-Rupture Ductility Data for Service Exposed Elbows (Test Conditions: 1150 F; 50 KSI)**

| Heat no. | Location of specimen | Rupture life (hr) | Elong. % | R.A. % |
|---|---|---|---|---|
| 806286 | plate | 11.0 | 40 | 54 |
| 806286 | plate | 5.2 | 40 | 51 |
| 806286 | plate | 15.4 | 38 | 56 |
| 806286 | plate | 29.2 | 43 | 55 |
| 806286 | transweld | 4.1 | 15 | 20 |
| 806286 | transweld | 8.1 | 11 | 13 |
| 806286 | transweld | 23.3 | 14 | 15 |
| 2813 | plate | 122.9 | 16 | 22 |
| 2813 | plate | 100.0 | 13 | 17 |
| 2813 | transweld | 15.1 | 13 | 17 |
| 2813 | transweld | 5.9 | 18 | 17 |
| 2969 | plate | 286 | 22 | 30 |

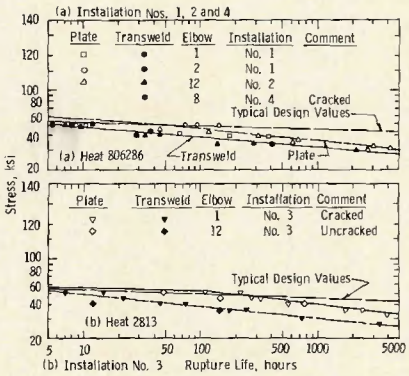


Fig. 21—Stress-rupture data of service-exposed material (temp 1150F) (left)

Fig. 22—Stress-rupture data of service-exposed material (temp 1150F) (below)

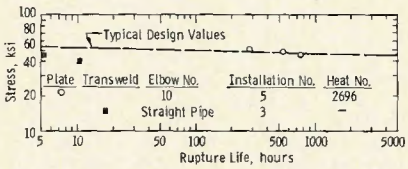


service exposed materials was significantly less than that of the nonservice exposed material, except in the case of low carbon material (Heat Nos. 2569 and 2696).

### Stress-Rupture Properties

Stress-rupture data from service exposed material are shown in Figs. 21 and 22, together with the typical design, stress-rupture curve at 1150F. In general, for all heats investigated, the original acceptance data are in good agreement with the design data. Therefore, the design data (dashed lines in Figs. 21 and 22) are used in this investigation as typical. Typical values of stress-rupture ductility are presented in Table 4.

Figure 21a shows the data for all tested elbows made from Heat No. 806286. The slope of the curve through the points for the plate material is about the same as that of the curve through the points for the transweld material, indicating that the rate of decrease of rupture strength is about the same for both cases. The same observation is true for Fig. 21b, which shows the data for Heat No. 2813. For the case of Heat No. 806286, there is a difference of about five times in the rupture life between transweld and plate values, and for the case of Heat No. 2813, the difference is about one order of magnitude. For both cases, the transweld values were lower.

Figure 22 shows the data for the transweld test conducted for the circumferential weld on the straight pipe of Installation No. 3 and the data for the service exposed elbow made from Heat 2696 (low carbon heat, 0.031%C). The data for the straight pipe indicate properties which are significantly lower than typical, while the data for Elbow No. 10, Installation No. 5, are about typical.

Several combination (plain bar-notch bar) specimens made from base material, Elbow No. 12, Installation No. 2, and Elbow No. 1 of Installation No. 3, were tested. All of these specimens broke in the plain bar section, indicating that the base material is notch insensitive.

## Fractographic Examinations

Electron microscope fractographic examinations were performed on several replicas made of portions of the cracks in five of the elbows involved in this investigation. Two-stage plastic-carbon replicas were used.

Fractographic examination of the small, internal crack in Elbow No. 10, Installation No. 5, confirmed that severe oxidation had occurred and that the degree of oxidation was uniform across the entire crack surface (of the portion originally present in the elbow). The oxidation was sufficiently severe to totally destroy the fracture features. In the surrounding areas (portions broken in the laboratory), the fracture was composed entirely of unoxidized, elongated dimples which is typical of ductile overload fracture. No evidence of stress-rupture fracture propagation of the crack could be found.

The fractographic examinations of cracks in the other four elbows further verified that the cracks were intergranular (except in the ductile overload or shear portions). In most of the intergranular areas, the oxidation had completely destroyed the fine crack features, leaving only an appearance of fine scales or small facets. Exceptions were noted near the tips of the intergranular (stress rupture) portions where the crack had been exposed to the steam environment for only relatively short periods. The amount of oxidation was progressively heavier at greater distances from the tips of the stress-rupture cracks. As discussed later, these oxidation gradients were used to estimate the crack growth rates of several of the stress-rupture cracks.

The overload portions of the cracks in all four elbows consisted mostly of dimpled rupture, with the exception of a few areas. The dimples were a mixture of elongated (shear) and equiaxed (tensile) types, and a wide range of sizes was evident. Some typical cases are shown in Fig. 23. Some intergranular separation had occurred, an example of which is also shown in Fig. 23, indicating that an extensive creep damage occurred throughout this area. Many small particles are present on the grain boundary surface shown in Fig. 23, and many impressions are present where particles appear to have pulled out (the particles are probably attached to the mating surface). This appearance suggests that decohesion of the boundaries of the precipitate (at the grain boundaries) and the matrix has occurred.

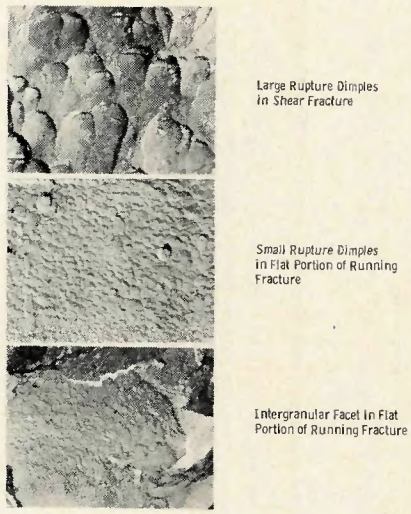


Fig. 23—Selected portions of surfaces in fast crack in elbow no. 1, installation no. 3. Mag: 2700X

Gradients in the degree of oxide attack were observed on the surfaces of the stress-rupture cracks. Various cracks in the four elbows were selected for further exploration to try to determine crack growth rates. A sufficient number of electron microscope fractographs were taken on each of these replicas to form a complete montage running from the dimpled rupture, across the interface, to a distance of 0.011 in. to 0.030 in. (depending on the sample) along the surface of the stress-rupture crack. The montage in each instance was long enough to illustrate the complete gradient of distinguishable features caused by the oxidation. Portions of a few typical areas from one of the cracks are shown in Fig. 24. In each case, the facets of the intergranular cracks near the intergranular-transgranular transition were relatively smooth, but they exhibited some oxidation products. At large distances away from the interfaces, toward the origin, the cracks exhibited a fine faceted appearance indicative of

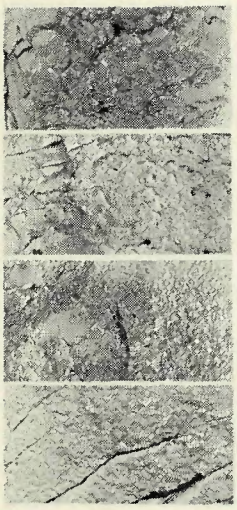


Fig. 24—Portions of surface of 0.24 in. deep stress-rupture crack in elbow no. 12, installation no. 2. Mag: 2080X

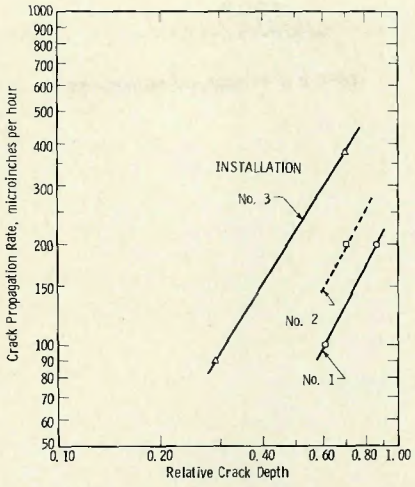


Fig. 25—Relationship of crack propagation rate with relative crack depth (ratio of crack depth to wall thickness) for stress-rupture cracks for various elbows

severe oxidation. At intermediate distances, a fine scale-like appearance prevailed which is characteristic of an intermediate degree of oxidation.

The differences in the relative amounts of oxidation of the cracks at the various locations are assumed to be due to the differences in time the various portions of the crack surfaces were exposed to the steam environment (namely, the time required for the crack front to progress from that location to the position just prior to the onset of the overload fracture or shutdown of the turbine). The crack surface appearances of cracked elbows at various locations were compared with laboratory produced cracks which had been exposed to a steam environment (simulating service conditions) for known periods of time. Thus, the times that the various portions of the service cracks had been exposed were estimated, and the propagation rates of the cracks were then calculated.

In Fig. 25, the logarithms of the crack growth rates of the various cracks are plotted as a function of relative crack depth (crack depth divided by nominal wall thickness). In this figure, a straight line is drawn through the two points for the two Installation No. 3 cracks and another through the Installation No. 1 cracks (one each in Elbow Nos. 8 and 11). In both instances, the slope of the lines is close to 2.0. A dashed line of a slope of 2.0 is shown through the point for the crack in Installation No. 2. Figure 25 shows that, for comparable crack lengths, the crack propagation rate is highest for the Installation No. 3 elbow and lowest for the Installation No. 1 elbows.

Rough estimates of the time necessary for propagation of the stress-rupture cracks from about 5% of the wall thickness to about 80% of the wall thickness was made for the elbows in each station as 7000 hours, 5000 hours, and 2500 hours for Installation Nos. 1, 2, and 3, respectively. These estimates were based on linear extrapolations of the lines in Fig. 25 relating crack propagation rates and crack depths.

## Discussion

The visual, macrographic, metallographic and fractographic examinations revealed that in each of the cracked elbows, except for Elbow No. 10 of Installation No. 5, the cracks were intergranular and had propagated quite slowly (at least for the initial portions). Multiple crack initiation (sometimes subsurface), branching, and grain boundary separation ahead of the main crack were typical. These features are typical of stress-rupture cracks. Since crack initiation was internal, in at least some instances, corrosion can be eliminated as contributing to the cracking.

In most cases the preferred location for cracking was the heat-affected zone of the base metal adjacent to the weld metal. The preference for this location over the weld metal, however, was apparently slight because weld cracking was observed in several cases.

The crack in Elbow No. 10 of Installation No. 5 was clearly different from all of the other cracks examined. This crack was completely transgranular and confined to the center of the weld; thus, it was not a stress-rupture crack as were the cracks in the other elbows which were investigated. Oxidation of fracture surface indicated that this crack must have been exposed to oxygen at a high temperature. This could not have occurred during service because the crack was completely internal. Furthermore, the uniformity of oxidation shows that the crack had not been propagating in service. The only time exposure of the crack surface to an oxygen-containing environment could have occurred is during welding, i.e., between the time that the root pass was made and the O. D. beads were deposited. Thus, the crack in Elbow No. 10 of Installation No. 5 was a manufacturing defect which did not lead to failure.

The results of the metallographic examination and mechanical properties determination for the cracked (stress-rupture cracks) components indicate that the high carbon materials used to manufacture these components are unstable at the service conditions. Heavy carbide precipitation occurs during service as shown in Fig. 17. The precipitation phenomenon appears to be restricted to the grain boundaries, twin boundaries and prior grain boundaries, and in the HAZ and weld metal the carbides formed an almost continuous film. This precipitation phenomenon was accompanied by a significant decrease of the stress-rupture strength of the material as shown in Fig. 20. For the case of Heats 806286 and 2813 the stress-rupture strength for 3000 hours life decreased by 16 ksi and 14 ksi, respectively (about 30% decrease) for service exposed material and the rate of decrease of failure stress to failure time ($\Delta\sigma$failure/$\Delta t$failure) is about four times greater for the service exposed material.

The noncracked components (either components with no cracks or with cracks other than stress-rupture cracks) can be divided in two groups, depending on the carbon content of the material. One group is the high carbon material ($C \geqq 0.048\%$) and the second group the low carbon material ($C \leqq 0.031\%$). The high carbon components have the same microstructural characteristic and mechanical properties as those described in the previous paragraph for cracked components. Of particular interest in Elbow No. 12, Installation No. 3 (a noncracked elbow), which was manufactured at about the same time and from the same plate as Elbow No. 1 of the same Installation (a cracked elbow). These two elbows were found to have the same microstructure characteristics and mechanical properties.

The low carbon components were

found to be mostly microstructurally stable (Fig. 17) with some moderate amount of precipitation present for the components with carbon contents close to 0.030%. This precipitation could have been present prior to service and it was determined to have essentially no effect on the stress rupture properties of the material, Fig. 22. These observations are based on available data, therefore, they refer only to the service time accumulated to the time of removal from service.

In all elbows and pipe investigated, stress-rupture cracking occurred only in high carbon material. Thus, at least for the service times investigated, high carbon appears to be a necessary although not sufficient condition for stress-rupture cracking. Proof that high carbon content is not the only factor required for cracking is that several high carbon elbows were examined and found to be free of cracks.

In most cases, stress-rupture cracks occurred only in portions of the elbows or pipe near extensive O.D. rewelded areas. In most cases, rewelding had been done by depositing several beads of weld metal along the O.D. surface, forming extensive weld overlays. In the case of the straight pipe, rewelding had been done after chipping out material in the vicinity of defective areas.

A few of the individual cracks appeared to have initiated at an area not closely associated with an extensive O.D. weld repair. Most of these cracks were in heat-affected zones of the base metal either at the opposite side of the weld at which I.D. weld repairs had been made or within about 1 in. of an O.D. weld repair. Only one exception was noted, i.e., the crack in Elbow No. 7 of Installation No. 4. In this instance, a crack initiated in the intrados about $^1/_2$ in. from the end of the elbow. Although this area appeared to be free of weld repairs, it was an area adjacent to the intersection of the intrados weld and the circumferential weld between Elbows 7 and 8 (see Fig. 8). The effect of the circumferential weld on the already existing intrados weld may well have been similar to the effect of a weld repair.

The implication of the association of stress-rupture cracks with rewelded regions (including intersecting welds) is that crack initiation is probably associated with the heat input from rewelding, or nearby welding, causing grain growth and sensitization (carbide precipitation).

## Conclusions

1. The cracks described herein are associated with welded joints and occur in the heat-affected zone, in the weld metal, or in the interface between weld and heat-affected zone.

2. All cracks, except one, were of the stress-rupture type. The exception was a manufacturing defect which did not propagate in service.

3. Crack lengths, depths, and separation widths are sufficiently large before reaching full wall thickness depths that they can be detected by existing field radiographic techniques.

4. The use of check analyses for plate quality control is necessary at least for carbon and silicon.

5. All stress-rupture cracks observed are associated with plates rolled from heats having more than 0.048%C on check analyses.

6. The high carbon material was significantly microstructurally unstable under the turbine operating conditions within the service time periods accumulated (high C $\geq$ 0.048% plate and $>$ 0.028% weld).

7. Mechanical properties of high carbon plate material (high C plate $\geq$ 0.048%) degrade with time at service conditions, the degradation being accelerated by development of $M_{23}C_6$ type precipitates at the grain boundaries.

8. Low carbon content heats are essentially microstructurally stable (low C $\leq$ 0.031% plate).

9. Transweld properties of joints are generally lower than those of the plate material.

10. All stress-rupture cracks examined occurred at rewelded areas, including intersecting welds.

11. The high carbon uncracked elbows examined contained no weld repairs.

12. Corrosion was not a factor in the initiation of cracks.

*Acknowledgements*

The authors thank J. Shinefield and W. Jeitner for their cooperation in different phases of this project; T. Busch, H. Rankin, B. Pilla, and A. Lindemanis for their cooperation in metallographic work; and L. Wagner and B. Hasiuk for some of the stress-rupture data.

J. Coles prepared the fractographic replicas, J. R. McDowell conducted the autoclave steam tests, and B. J. Sauka made the low-pressure oxidation tests and prepared the fractographic layouts. C. B. Brenneman, Jr., made the X-ray studies, which were evaluated by J. K. White. Check chemical analyses were made by J. Rudolph, M. A. Fulmer, K. Guardipee, S. Oliverio, C. L. Page, and J. Penkrot. Metallography was done by R. M. Slepian, et al.

Dr. F. C. Hull reviewed the manuscript for technical and historical accuracy. All elbow and pipe layouts for specimens were made by W. R. Kuba and P. T. Ehrhardt.

*References*

1. F. C. Hull and R. Stickler, "Effect of Nitrogen, Boron, Zirconium, and Vanadium Upon Microstructures, Tensile and Creep Rupture Properties of a Cr-Ni-Mn-Mo Stainless Steel," Joint International Conference on Creep, New York, Aug. 25 to 29, 1963. Paper No. 43.

2. F. C. Hull, "A High-Strength Weldable Steel for Elevated-Temperature Service," ASTM-STP No. 369, 1965, p. 88.

3. J. A. Isasi, R. C. Bates, and J. Heuschkel, "Analysis of Cracks in Welded Elbows," ASME, First National Congress on Pressure Vessels and Piping, May 1971, Paper No. 71-PVP-32.

4. S. K. Chan, M. J. Manjoine, and C. Visser, "Analysis of Stresses in Pressurized Welded Pipe in the Creep Range," ASME, Ibid., Paper No. 71-PVP-66.